Simultaneous H_2 Production with Carbon Storage by Enhanced Olivine Weathering in Laboratory-scale: An Investigation of CO_2 Effect

Jiajie Wang*, Kengo Nakamura, Noriaki Watanabe, Atsushi Okamoto and Takeshi Komai
Graduate School of Environmental Studies, Tohoku University, Aramaki, Aoba-Ku, Sendai, Japan

Keywords: H_2 production, CO_2 storage, Rock-water reaction, Olivine, CO_2-rich.

Abstract: Hydration of olivine ($(Mg,Fe)_2SiO_4$) potentially offers significant H_2 supply. However, because of the low Fe(II) dissolution rate, H_2 production rate is poorly limited. In the present study, to investigate the CO_2 effect on H_2 generation and minerals evolution, CO_2-rich (0.5 mol/L $NaHCO_3$) reaction condition was created in the ongoing olivine hydration experiment. H_2 production was continuing with a slight increasing rate after CO_2 addition. Results indicate CO_2-rich hydrothermal reaction condition (300 ºC, 10 MPa) promoted both olivine and brucite ($Mg,Fe(OH)_2$) dissolution, which led to additional Fe(II) releasing, and consequent H_2 generation. CO_2 was simultaneous hydrogenated to formic acid (HCOOH) by generated H_2 and carbonated to magnesite ($MgCO_3$). 0.52 mol of CO_2 was trapped in per kg of olivine in 72 h. This study suggests simultaneous multiple energy productions and CO_2 storage can be realized by olivine weathering process when using a CO_2-rich hydrothermal condition.

1 INTRODUCTION

In 2016, the atmospheric carbon dioxide (CO_2) is 403.3 ppm, having increased by 45% compared with the pre-industrial level of 280 ppm and still increasing at a rate of 2 ppm per year (NOAA, 2016). Among which, up to 65% were attributed to fossil fuel combustion (Kularatne et al., 2018). Control of global warming and the exploration of CO_2-free energy sources are the main challenges in the 21st century. Hydrogen (H_2) is a clean CO_2-free energy carrier. However, most current H_2 production processes (e.g., steam reforming of CH_4) need high temperature, which was supported by the combustion of fossil fuels. Also, this process generates CO_2 as a reaction product (Malvoisin et al., 2013).

In recent years, H_2 was discovered from a variety of geologic fluids. It is commonly produced during the hydration of rocks, owing to the oxidation of reduced Fe present in the mineral (Kelley, 1996; Lollar et al., 2008) at hydrothermal conditions. Olivine ($(Mg,Fe)_2SiO_4$) is the predominant mineral of ultramafic rock, the hydration of olivine (also called serpentinization) potentially offers significant H_2 supply. However, the rate of H_2 generation from olivine hydration is poorly limited. The low H_2 generation rate is partially attributed to the low olivine dissolution rate, which can be enhanced by varying reaction conditions, such as elevating reaction temperature. Research reported the optimum temperature H_2 production from olivine hydration was 300-400 ºC (Berndt et al., 1996; McCollom and Seewald, 2001). On the other hand, dissolved Fe(II) prone to be incorporated into brucite ($Mg,Fe(OH)_2$), the secondary mineral of olivine hydration. This process decreases dissolved Fe(II) in the fluid, thus fewer Fe(II) can be oxidized, which severely suppresses H_2 yield (Klein et al., 2009).

The presence of bicarbonates (HCO_3^-) can promote olivine and brucite dissolution (Matter and Kelemen, 2009; Gerdemann et al., 2007; Harrison et al., 2013). High concentrations of HCO_3^- in solution plays as a buffer to maintain relatively weakly alkaline pH, which has an enhancement in olivine dissolution. (Harrison et al., 2013) proposed HCO_3^- can significantly promote brucite dissolution. Thus, the CO_2-rich condition potentially enhances Fe(II) being dissolved, then H_2 production will be accelerated. Although researches concerning hydrocarbon generation based on serpentinization process have used $NaHCO_3$ as the source of inorganic carbon, the chemical reactions between HCO_3^- and

Wang, J., Nakamura, K., Watanabe, N., Okamoto, A. and Komai, T.
Simultaneous H2 Production with Carbon Storage by Enhanced Olivine Weathering in Laboratory-scale: An Investigation of CO2 Effect.
DOI: 10.5220/0008186000830087
In *The Second International Conference on Materials Chemistry and Environmental Protection (MEEP 2018)*, pages 83-87
ISBN: 978-989-758-360-5

minerals was rarely considered, partially because of the extremely low concentration of HCO_3^- (Berndt et al., 1996; McCollom and Seewald, 2001).

Olivine carbonation process also occurs with the presence of CO_2. The CO_2-rich condition, typically 0.64 M $NaHCO_3$, favors olivine carbonation at < 200 °C (Matter and Kelemen, 2009; Gerdemann et al., 2007). However, previous studies mainly focus on olivine serpentinization or carbonation separately, because they occur at different temperature range. Whether serpentinization and carbonation can proceed simultaneously, and the effects of CO_2-rich fluid on serpentinization and H_2 production are less clear.

This study was designed to investigate the changes in H_2 generation, fluid chemistry and secondary minerals generations after CO_2-rich fluid addition. The role of CO_2 on olivine serpentinization and carbonation were revealed, as well as the reactions for dissolved carbon: hydrogenated or mineralized. Gas, fluid and mineral samples were withdrawn during the reaction to reveal the mineralogical changes over time.

2 MATERIALS AND METHODS

2.1 Materials

Purchased olivine grains were chosen for experimental investigation, which was collected from Damaping (China). Then olivine was ball-milled (Pulverisette 6, Fritsch) to diameter <45 μm. The composition of the olivine was measured using Electron probe micro-analyzer (EPMA) and was defined as $Mg_{1.8}Fe_{0.2}SiO_4$. The effect of CO_2 on olivine weathering was investigated using $NaHCO_3$ (Kanto Chemical, Japan).

2.2 Experimental Setup and Analytical Methods

Experiments were performed in a closed-batch reactor made of Hastelloy-C with an internal volume of 170 mL (Figure 1). In each experiment, 100 mL slurry prepared with 5±0.01 g of olivine powders and Milli-Q water was poured into the reactor. Then the reactor was closed and purged with N_2 gas for 10 minutes to remove dissolved O_2 in the solution and the upper headspace. Then air outlet was closed and N_2 gas continues to be injected to reach a certain pressure. The reactor was well sealed to increase the temperature to 300 °C, with the final pressure reached 10 MPa. After 72 h reaction, the reactor was opened and $NaHCO_3$ was added to create CO_2-rich (0.5 mol/L $NaHCO_3$) reaction condition. Then the reactor was sealed and the original reaction conditions (300 °C and 10 MPa) were reset. Gas, liquid and solid samples were withdrawn along the reaction via sampling tubes. Solid samples withdrawn at the reaction time of 72 and 144 h were named as O72 and O72-C72, respectively. After 144 h, experiments were stopped by reducing the temperature of the reactor using recirculated cooling water. The mineral powder was filtered and dried at 50 °C for 24 h in an oven before further analysis.

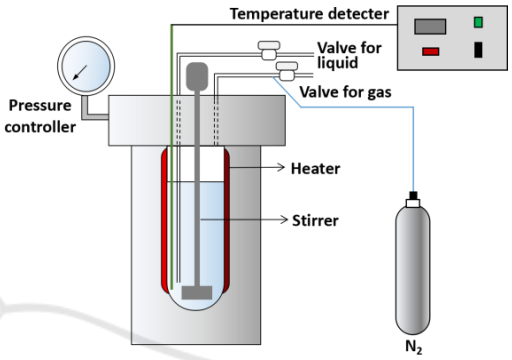

Figure 1: Schematic diagram of the experimental set-up.

Liquid samples were analyzed using ion chromatography (IC; 761 Compact IC, Metrohm, Switzerland) coupled with a Metrosep Organic Acids column (Metrohm, Switzerland), and Inductively Coupled Plasma equipped with an Atomic Emission Spectrometry (ICP-AES). Gas species were analyzed using gas chromatography (GC; GC-3200, GL Science, Japan) equipped with a thermal conductivity detector (TCD). Mineral compositions and crystalline structures of the minerals were measured using XRD (Multiflex, Rigaku, Japan) with Cu Kα radiation (λ= 1.54 Å) operated at 40 kV and 20 mA, and with a 2θ step size of 0.02° from 10° to 45°. The surface morphologies of the minerals were observed using scanning electron microscopy (SEM; SU-8000, Hitachi, Japan). Thermogravimetric analyses (TGA) of the solid samples were performed using a thermos-dilatometer (Thermo plus EVO TG 8120, Rigaku, Japan). The temperature was increased from room temperature to 1000 °C at a rate of 10 °C per minutes. The H_2O contents of brucite and serpentine ($Mg_3Si_2O_5(OH)_4$), CO_2 contents of magnesite ($MgCO_3$) could be determined separately from the weight loss observed in different temperature ranges. Then the mass losses due to different minerals could be identified, and the final mineral composition was estimated.

3 RESULTS AND DISCUSSION

3.1 Energy Production

During the reaction, gas and liquid samples were withdrawn at the reaction time of 3, 24, 72, 75, 96, 120 and 144 h. Gaseous H_2 and liquid HCOOH were experimental detected as the main products in the present study. Products yields were measured three times, and the average ones are summarized in Figure 2. CH_4 was also detected after 72 h reaction. However, the concentration was too low (several µmol) to be quantified with sufficient accuracy.

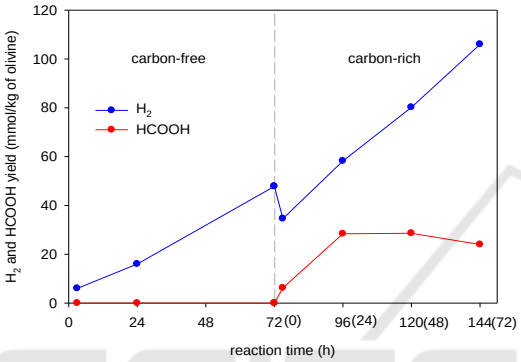

Figure 2: H_2 and HCOOH productions as function of time.

In the first 72 h, the slurry was CO_2-free. H_2 yield increased to 47.8 mmol/kg of olivine with olivine hydration proceeding, suggesting that Fe(II) dissolved from olivine was oxidized to Fe(III). HCOOH was not detected in this stage, indicating dissolved carbon was almost removed out from solution via N_2 bubbling process. After 72 h reaction, $NaHCO_3$ was added into the reactor to create a concentration of 0.5 mol/L. The accumulated H_2 yield increased to 106.0 mmol/kg of olivine after reaction for another 72 h. The continuous generation of H_2 in the CO_2-rich condition indicates that Fe(II) oxidation was not retarded. The average H_2 production rate was increased from 0.61 mmol/kg·h before $NaHCO_3$ addition to 1.03 mmol/kg·h after $NaHCO_3$ addition. (Klein and McCollom, 2013) reported the CO_2 addition would severely retarded H_2 production from olivine because of dissolved Fe(II) was easier to be incorporated into magnesite rather than be oxidized. Compares it with the present study, the reaction temperature may play an important role on judging the CO_2 effect on H_2 production. Their reaction temperature is 230 ºC while that of the present study is 300 ºC. HCOOH was generated in the first 3h after $NaHCO_3$ addition and reached stable at 28.4 mmol/kg of olivine after 24 h. CH_4 concentration did not increase even at the CO_2-rich condition with higher HCOOH and H_2 concentrations.

3.2 Fluid Chemistry

Fluid compositions of the samples withdrawn during the reaction are summarized in Figure 3. During the first 72 h reaction in carbon-free condition, pH of the slurry decreased from initial 10.62 to 9.84. Dissolved $SiO_{2(aq)}$ concentration increased from initial 0.34 to 0.40 mol/L in the first 24 h, then followed by a slight decrease to 0.23 mmol/L. Mg^{2+} concentration increased from initial value 0.08 to a plateau of 0.73 mmol/L, whereas Ca^{2+} concentration increased slightly from initial value 0.04 to 0.06 mmol/L. The much smaller increase in Ca^{2+} concentration is attributed to the low Ca composition in initial olivine particles. As the reaction progress, which was attributed to olivine dissolution.

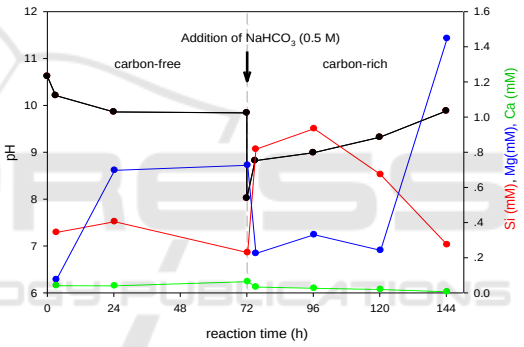

Figure 3: Fluid composition as a function of time.

The addition of $NaHCO_3$ caused rapid changes in the fluid chemistry. Solution pH decreased from 9.84 to 8.02 immediately because of the buffering of $NaHCO_3$. In the subsequent reaction, the pH increased to 9.49 gradually with the reaction time reaching 144 h. The increase of pH was partially attributed to the dissolution of olivine particles. With the addition of $NaHCO_3$, $SiO_{2(aq)}$ concentration increased significantly from 0.23 to 0.82 mmol/L in 3 h, which indicates the enhancement on olivine dissolution (Klein and McCollom, 2013; Gadikota et al., 2014). As the reaction process, $SiO_{2(aq)}$ concentration eventually decreased again to 0.27 mmol/L. Mg^{2+} concentration decreased immediately from 0.73 to 0.22 mmol/L, whereas Ca^{2+} concentration decreased from 0.06 to 0.03 in 3 h after the addition of $NaHCO_3$. It indicates the carbonation process conducted quickly after CO_2 was added. At the last 24 h of the reaction, the Mg^{2+} concentration

increased sharply to 1.45 mmol/L, infers the retarded carbonation process.

3.3 Mineral Changes

Solid after reactions were analysed using XRD to identify mineral compositions. The results are shown in Figure 4. The main mineral products before carbon injection are serpentine, brucite and magnetite (Fe_3O_4). Evident serpentine peaks were observed at 12.2°, 19.4° and 24.5° after 72 h reaction in CO_2-free condition. It infers serpentinization was the main process for olivine weathering at this stage. Peaks at 18.8° and 38.1° are referred to brucite (Schaef et al., 2011). Magnetite peak was found at 30.2°. No magnesite peak was detected. After creating a CO_2-rich condition in the reactor and continuing the reaction for another 72 h, stronger serpentine peaks were observed from the solid sample. It indicates the promoted serpentine generation. The peak occurred around 32.8° belongs to magnesite (Rahmani et al., 2016), which indicates the carbonation process. In addition, brucite content was severely decreased with much smaller brucite peaks be observed.

SEM imaging has revealed a clear evolution of morphology of crystal face during olivine weathering process. The dominant serpentine polymorph found is chrysotile. Before the CO_2 addition, chrysotile fibers have a diameter of 10-100 nm and are less than 1 μm in length (Figure 5(a)). Brucite and few magnetites were generated with several μm in size (Figure 5(b, c)). After reacting in CO_2-rich condition for another 72 h, serpentine fibrous became longer with more than 2 μm in length (Figure 5(d)). Brucite was hardly observed. Brucite potentially incorporates Fe(II). The addition of $NaHCO_3$ in present study promoted Fe(II)-bearing brucite dissolution, thus enhanced Fe(II) being released, which potentially accelerated H_2 generation. More magnetite particles were observed according to SEM imaging (Figure 5(e)). However, the changes in mineral yield cannot be determined, since the observed area using SEM observations is very limited. Magnetite is the secondary mineral contains Fe(III), the formation of magnetite infers the oxidation of Fe(II). In addition, magnetite is a well-studied catalyst for CO_2 reduction, which particular catalyzes CH_4 generation. However, in the present study, CH_4 yield was low, the reason still needs to be explored. Magnesite, the main products of CO_2 mineralization, was generated after $NaHCO_3$ addition, as to be shown in Figure 5(f) with rhomb shape.

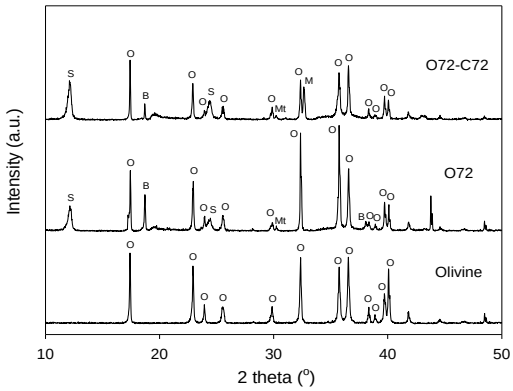

Figure 4: XRD patterns of olivine, olivine after 72 h reaction in CO_2-free condition (O72) and after an additional 72 h reaction in CO_2-rich condition (O72-C72). O: olivine, S: serpentine, B: brucite, M: magnesite, Mt: magnetite.

Table 1: TGA results of mineral compositions.

Sample	Product amount (wt.%) from TGA			
	Serpentine	Magnesite	Brucite	Olivine
O72	12.65	0.00	0.45	86.76
O72-C72	31.05	4.07	0.00	64.33

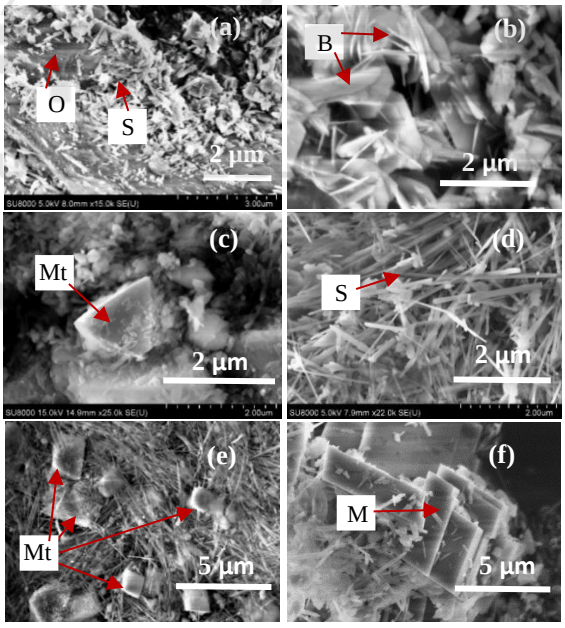

Figure 5: SEM images of minerals after reacting for 72 h (a, b, c) and 144 h (d, e, f). O: olivine, S: serpentine, B: brucite, Mt: magnetite, M: magnesite.

To quantify the mineral compositions after reactions, TGA was used. The calculated results are shown in Table 1. The weight percent of serpentine generated in the CO_2-free condition in 72 h is 12.65 wt.%. After reacting in CO_2-rich condition for

another 72 h, serpentine composition increased by 18.40 wt.%. It indicates serpentinization process was slightly promoted in the presence of CO_2. Magnesite was generated in the second stage of the experiment with CO_2. The yield was 4.07 wt.% of solid collected after 72 h reaction, equivalent to trapping of 0.52 mol of CO_2 per kg of olivine. Brucite was consumed after CO_2 addition as no weight loss belongs to brucite was detected in the O72-C72 solid sample.

4 CONCLUSIONS

The present study traced the changes in H_2 yield, fluid chemistry and minerals after CO_2 addition as a function of time. H_2 generation was continuing at the CO_2-free and CO_2-rich condition. The production rate was increased slightly after the addition of $NaHCO_3$. Olivine and brucite dissolution were accelerated in CO_2-rich condition, which may be attributed to pH decrease caused by $NaHCO_3$ addition. The dissolution of Fe(II)-contained brucite contributed Fe(II) releasing, thus promoted H_2 production. Our experiment results suggest simultaneous energy production and CO_2 storage can be realized when using CO_2-rich hydrothermal condition in olivine weathering process.

ACKNOWLEDGEMENTS

The authors thank Kawabe Yoshishige in AIST (Japan) for helping ICP-AES analysis. The authors also thank reviewers who gave helpful suggestions. This work was supported by JSPS KAKENHI Grant Number JP18J12695.

REFERENCES

Berndt, M., Allen, D. and Seyfried, W., 1996. Reduction of CO_2 during serpentinization of olivine at 300 °C and 500 bar. *Geology*, 24(4), pp.351-354.

Gadikota, G., Matter, J., Kelemen, P. and Park, A., 2014. Chemical and morphological changes during olivine carbonation for CO_2 storage in the presence of NaCl and $NaHCO_3$. *Physical Chemistry Chemical Physics*, 16(10), pp.4679.

Gerdemann, S., O'Connor, W., Dahlin, D., Penner, L. and Rush, H., 2007. Ex Situ Aqueous Mineral Carbonation. *Environmental Science & Technology*, 41(7), pp. 2587-2593.

Harrison, A., Power, I. and Dipple, G., 2012. Accelerated Carbonation of Brucite in Mine Tailings for Carbon Sequestration. *Environmental Science & Technology*, 47(1), pp. 126-134.

Kelley, D., 1996. Methane-rich fluids in the oceanic crust. *Journal of Geophysical Research: Solid Earth*, 101(B2), pp. 2943-2962.

Klein, F. and McCollom, T., 2013. From serpentinization to carbonation: New insights from a CO_2 injection experiment. *Earth and Planetary Science Letters*, 379, pp. 137-145.

Klein, F., Bach, W., Jöns, N., McCollom, T., Moskowitz, B. and Berquó, T., 2009. Iron partitioning and hydrogen generation during serpentinization of abyssal peridotites from 15ºN on the Mid-Atlantic Ridge. *Geochimica et Cosmochimica Acta*, 73, pp. 6868-6893.

Kularatne, K., Sissmann, O., Kohler, E., Chardin, M., Noirez, S. and Martinez, I., 2018. Simultaneous ex-situ CO_2 mineral sequestration and hydrogen production from olivine-bearing mine tailings. *Applied Geochemistry*, 95, pp. 195-205.

Lollar, B., Lacrampe-Couloume, G., Voglesonger, K., Onstott, T., Pratt, L. and Slater, G., 2008. Isotopic signatures of CH_4 and higher hydrocarbon gases from Precambrian Shield sites: A model for abiogenic polymerization of hydrocarbons. *Geochimica et Cosmochimica Acta*, 72(19), pp. 4778-4795.

Malvoisin, B., Brunet, F., Carlut, J., Montes-Hernandez, G., Findling, N., Lanson, M., Vidal, O., Bottero, J. and Goffé, B., 2013. High-purity hydrogen gas from the reaction between BOF steel slag and water in the 473–673 K range. *International Journal of Hydrogen Energy*, 38(18), pp. 7382-7393.

Matter, J. and Kelemen, P., 2009. Permanent storage of carbon dioxide in geological reservoirs by mineral carbonation. *Nature Geoscience*, 2(12), pp. 837-841.

McCollom, T. and Seewald, J., 2001. A reassessment of the potential for reduction of dissolved CO_2 to hydrocarbons during serpentinization of olivine. *Geochimica et Cosmochimica Acta*, 65(21), pp. 3769-3778.

NOAA, 2016. Trends in Atmospheric Carbon Dioxide.

Rahmani, O., Highfield, J., Junin, R., Tyrer, M. and Pour, A.B., 2016. Experimental Investigation and Simplistic Geochemical Modeling of CO_2 Mineral Carbonation Using the Mount Tawai Peridotite. *Molecules*, 21(353).

Schaef, H.T., Windisch Jr., C.F., McGrail, B.P., Martin, P.F., and Rosso, K.M., 2011. Brucite [$Mg(OH_2)$] carbonation in wet supercritical CO_2: An in situ high pressure X-ray diffraction study. *Geochimica et Cosmochimica Acta*, 75, pp. 7458-7471.